We demonstrated that adult hippocampal Wnt/β-catenin signalling triggers NeuroD1 expression (Kuwabara et al, 2009). NeuroD1, a basic helix-loop-helix (bHLH) transcription factor, has been shown to play an important role in both developing pancreas and brain (Liu et al, 2000; Miyata et al, 1999; Naya et al, 1997, 1995). NeuroD1-deficiency in mice causes severe diabetes and perinatal lethality because NeuroD1 is required for insulin gene expression (Naya et al, 1997, 1995). Similar to the loss of Wnt/β-catenin signalling (Lee et al, 2000), NeuroD1 deficiency during hippocampal development leads to a complete loss of DG formation in mice (Liu et al, 2000; Miyata et al, 1999). Despite their separate developmental origins, the gene expression programs for developing neurons and β cells are remarkably similar (Edlund, 2002; Habener et al, 2005). However, insulin expression in the adult brain and the underlying regulatory mechanism, have not been demonstrated.

Here, we provide evidence that adult granule neurons natively express insulin. This insulin expression during neuronal differentiation was observed not only in hippocampal NSCs (HPC NSCs) but also in adult NSCs isolated from the OB (OB NSCs). Wnt3 played an important role in up-regulating endogenous NeuroD1 expression, which in turn activated insulin gene expression by the direct association of NeuroD1 with the insulin promoter in both HPC and OB NSCs. Although the contribution of Wnt3 to insulin expression was apparent, inhibitory mechanisms also played a role. Insulin-like growth factor-binding proteins (IGFBPs), which acted as inhibitory factors of Wnt-mediated promotion, were up-regulated upon neuronal differentiation. In DB animals, IGFBP-4 expression was further up-regulated, whereas, Wnt3 and NeuroD1 expression declined. Importantly, adult HPC and OB NSCs derived from DB animals retained the ability to generate insulin-producing cells. *Ex vivo* culture with Wnt3a ligand and a neutralizing antibody against IGFBP-4 significantly promoted insulin production, and grafted adult HPC and OB NSCs from DB animals became efficient sources of *de novo* insulin biosynthesis *in vivo*. Our results confirm the strong functional similarity between adult neurons and β cells and suggest possible approaches to cell replacement therapy for diabetes.

RESULTS

Hippocampal neurons express insulin and C-peptide

We first investigated *insulin-1* mRNA expression in adult HPC by *in situ* hybridization. Positive *insulin-1* mRNA signals were detected at granule cell layers (GCL) in DG (Fig 1A; negative controls are shown in Fig S1A of Supporting information). Strong signals were observed in neuronal layers but were not found in cells at the inner layer of the DG where astrocytes and undifferentiated NSCs reside. Signals were also detected in CA1 and CA3 pyramidal neuron layers (Fig S1B of Supporting information).

The expression of insulin-1 protein in adult HPC and pancreas was examined in parallel by enzyme-linked immunosorbent assay (sandwich enzyme-linked immunosorbent assay; ELISA). Although the insulin expression level was significantly higher in the pancreas than in the brain (>10-fold), adult brain and HPC contained released insulin (Fig S2 of Supporting information). Insulin expression was also analysed immunohistochemically (IHC). Insulin-producing cells were clearly detected in granule neurons in DG, and these cells expressed β-tubulin III (TUJ1, Fig 1B). Insulin was expressed in the cell body and extensively in neurites extending from neurons (Fig 1B; molecular layer). Neurons in the CA1 pyramidal region, cortex and substantia nigra were also positive (Fig S3 of Supporting information). Adult pancreatic islet β cells were TUJ1+ (Fig S3B of Supporting information), suggesting similar gene expression between β cells and neurons. In DG neurons, *de novo* insulin production was confirmed by the simultaneous detection of C-peptide (Fig 1C), similar to that in pancreatic islets (Fig S3C of Supporting information). From these *in situ* hybridization, ELISA and IHC data, we confirmed that adult hippocampal neurons endogenously expressed insulin to a lesser extent than pancreatic islets.

Pancreatic α cells release Wnt3, and its level is decreased in diabetic rats

Because neurons produced insulin (Fig 1), we were interested in the niches that supported neuronal differentiation. Astrocytes define the HPC niche (Song et al, 2002), and astrocyte-secreting Wnt3 factors (Fig S4A of Supporting information) have instructive effects in promoting adult neurogenesis (Lie et al, 2005). Glial fibrillary acidic protein (GFAP) is an astrocyte marker, and GFAP-expressing (GFAP+) cells were detected in pancreatic α cells (Fig S4B of Supporting information). Interestingly, IHC revealed that the pancreatic GFAP+ cells co-localized with Wnt3+ cells (Fig 2A), indicating that α cells release the neurogenic Wnt3 as do hippocampal astrocytes.

In diabetes, deficits in insulin secretion influence the pancreatic endocrine system and HPC function (Stranahan et al, 2008). To determine Wnt3 expression under physiological changes, we compared the Wnt3+ cell population between wild-type and DB rats. In both streptozotocin (STZ)-induced type 1 DB and type II DB Goto-Kakizaki (GK) rats, marked reductions in Wnt3+ cells were observed in the pancreas Fig 2B, left; $p < 0.001$, data represent +s.d. $n = 6$ *per* group), which was also observed in the HPCs of DB rats (Fig 2B, right). Following the reduction in Wnt3+ cells in DB rats, the expression of *Wnt3* mRNA was down-regulated consistently in both pancreatic islets and the HPC (Fig 2C and D). Insulin, IGF-1 and IGF-2 were also down-regulated. Interestingly, IGFBP-4 expression was up-regulated in DB rats (Fig 2C and D).

A family of IGF-binding proteins (Firth and Baxter, 2002) modulates the bioactivity of IGF and impairs Wnt/β-catenin signalling (Zhu et al, 2008). The most potent canonical Wnt inhibitor in the IGFBP family is IGFBP-4 (Zhu et al, 2008). In diabetes, potent competitors (IGF-1 and IGF-2) of IGFBP-4 were down-regulated and the Wnt3 inhibitor IGFBP-4 was present in higher levels; further, the HPC and pancreas expressed lower levels of Wnt3.

Adult neural progenitor cells from the HPC and OB

Manipulating endogenous NSCs or transplanting the progeny of exogenously expanded neural progenitors may lead to

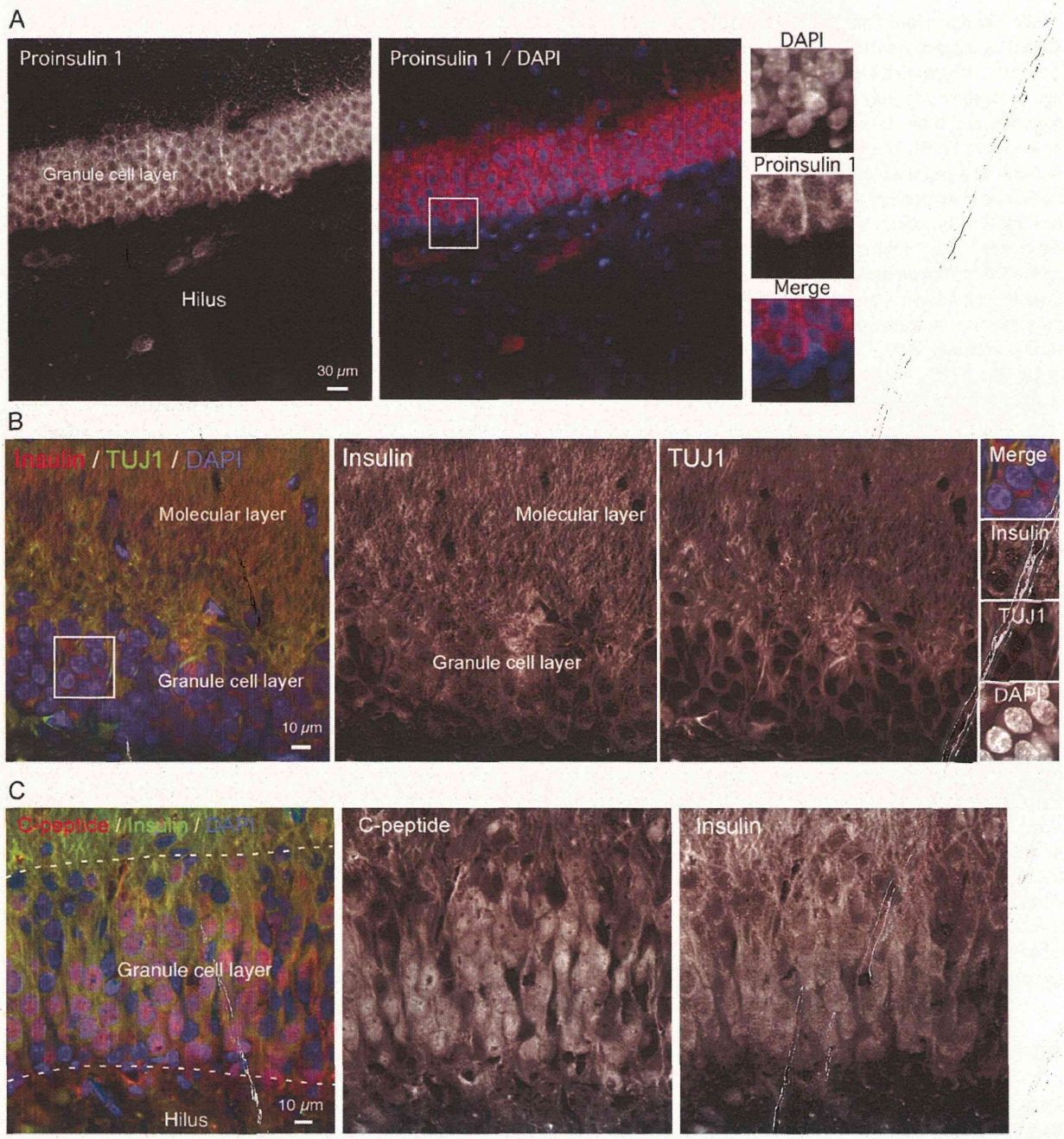

Figure 1. Adult hippocampal neurons express insulin.

A. *In situ* hybridization of proinsulin 1 mRNA in adult rat HPC. *In situ* hybridization of insulin and DAPI staining in the DG region are shown. Cells in the white square region are magnified and shown in separate panels at right. Proinsulin 1, red; DAPI, blue.

B. Immunohistochemistry analysis of insulin in DG of adult HPC. Insulin-immunoreactive cells (red) were detected in both the GCL and molecular layer of HPC, and they also expressed β tubulin III (TUJ1, green). Cells in the white square region are magnified and shown in separate panels at right. Insulin, red; TUJ1, green; DAPI, blue.

C. Detection of C-peptide in adult granule neurons in DG of HPC. C-peptide is generated when proinsulin is split into insulin and C-peptide. C-peptide, red; Insulin, green; DAPI, blue.

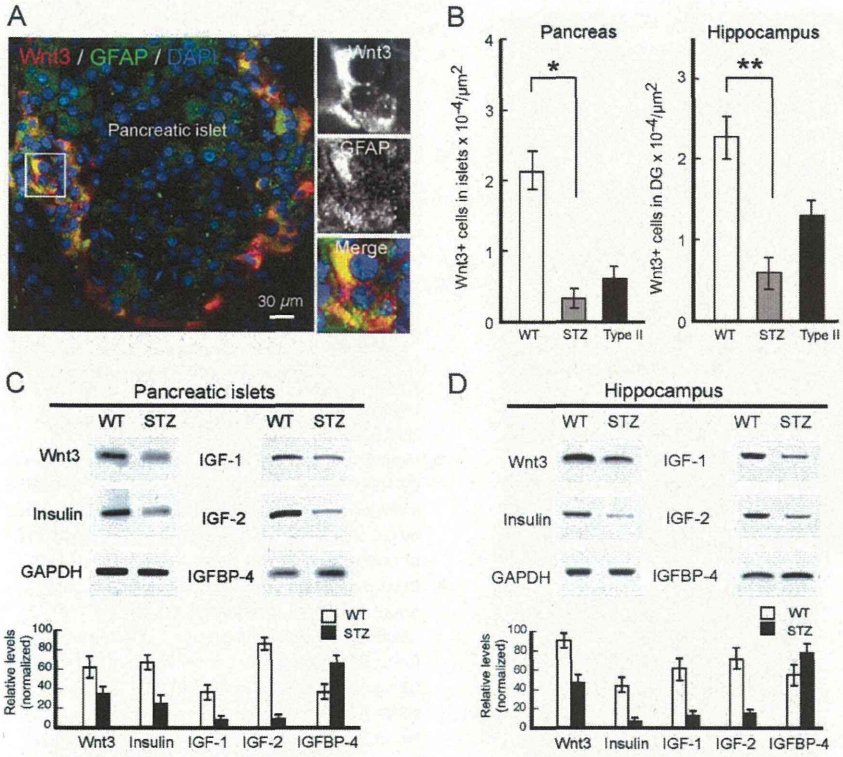

Figure 2. Wnt3, released from pancreatic α cells, decreases in diabetes.

A. Detection of Wnt3 in the pancreatic α cells expressing GFAP. A confocal image of IHC of Wnt3 and GFAP in adult pancreatic islet is shown. Cells in the white square region are magnified and shown in separate panels at right. Wnt3, red; GFAP, green; DAPI, blue.

B. Comparison of the number of Wnt3-positive cells in pancreas (left) and in DG of HPC (right) obtained from wild-type and diabetes rats. White bars, wild-type Fisher 344 rats (10-week old, male); grey bars, STZ-induced type I DB rats (10-week old, male); type II DB GK rats (10-week old, male). $^{*}p < 0.01$ and $^{**}p < 0.001$.

C. Comparison of mRNA levels of Wnt3, insulin, IGFs and IGFBP-4 between wild-type and DB animals (STZ-induced DB rats) in the pancreas.

D. Comparison of mRNA levels of Wnt3, insulin, IGFs and IGFBP-4 between wild-type and DB animals (STZ-induced DB rats) in the HPC. Relative levels of mRNA were normalized to GAPDH in the following Q-PCR analysis and are plotted at bottom.

successful cell replacement therapies for various diseases. The discovery of insulin expression in neurons prompted us to use adult NSCs without exogenous gene induction as sources of insulin-producing cells from the patient's own organs to treat diabetes. HPC NSCs are well established and have been studied extensively, whereas, OB NSCs are of potential interest because of their easily accessible location (Curtis et al, 2007; Liu and Martin, 2003; Pagano et al, 2000; Zhang et al, 2004).

HPC NSCs were round and retained this shape when expanded as a monolayer (Fig 3A, left). OB NSCs grew as heterogeneous forms with adherent property and neurosphere morphologies (Fig 3A, right). Under neuron differentiation conditions, the cell morphologies changed markedly: both HPC and OB NSCs extended prolonged neurites (Fig 3B). Gene expression profiles were measured using Agilent rat genome microarrays (Table 1 of Supporting information). HPC NSC, OB NSC and HPC and OB neuron expression profiles were grouped by hierarchical clustering, and correlation coefficients were computed for all pair-wise comparisons (Fig S5 of Supporting information). Both HPC NSCs and OB NSCs expressed the NSC marker *Sox2*, the radial glial cell marker *nestin* and the neural progenitor markers *Olig2* and *Sox1* (NSC lineage; Fig 3C). NSC marker gene expression was down-regulated in HPC and OB neurons (HPC Neu and OB Neu in Fig 3C), and neuronal marker gene expression was up-regulated (mature neuron marker; Fig 3C), indicating their successful commitment into neuronal lineages.

Importantly, *insulin-1* and *insulin-2* expression increased extensively in HPC and OB neurons (pancreatic genes; Fig 3C). IHC revealed that rat OB neurons were insulin+ natively (Fig S3D of Supporting information), consistent with the microarray data. *Pax3*, an early developmental stage neural crest marker was not detectable. Another neural crest marker, *Sox10*, was expressed in these cells, but the levels were unchanged upon neuronal differentiation. These data suggested that insulin was up-regulated in neurons derived from adult NSCs in both the HPC and OB and that its regulation in adult neuronal lineages could be distinguished from the commitment event in embryonic neural crest lineages.

In the pancreatic lineage, insulin gene expression is regulated by several transcription factors abundant in islets such as NeuroD1, neurogenin 3 Pdx1 and MafA (Melloul et al, 2002; Sander and German, 1997; Servitja and Ferrer, 2004). MafA and MafB are co-expressed in insulin+ β cells during embryogenesis, whereas, in the adult pancreas, only MafA is produced in β cells and MafB in glucagon+ α cells (Nishimura et al, 2006). Our microarray analysis revealed that neither HPC nor OB neurons expressed MafA, Pdx1 or neurogenin 3, which are necessary to activate the insulin gene in pancreatic β cell lineages. Quantitative real-time RT-PCR analysis confirmed that *insulin-1* mRNA induction was correlated with *NeuroD1* mRNA up-regulation in both the HPC and OB (Fig 3D). The *insulin-1* mRNA induction resulting from NeuroD1 siRNA transfection led to its down-regulation in neurons, whereas, *MafA*, *Pdx1* or *neurogenin 3* siRNAs had no influence (Fig 3E). These data suggested that *NeuroD1* expression is required for insulin expression in adult NSCs *in vitro*.

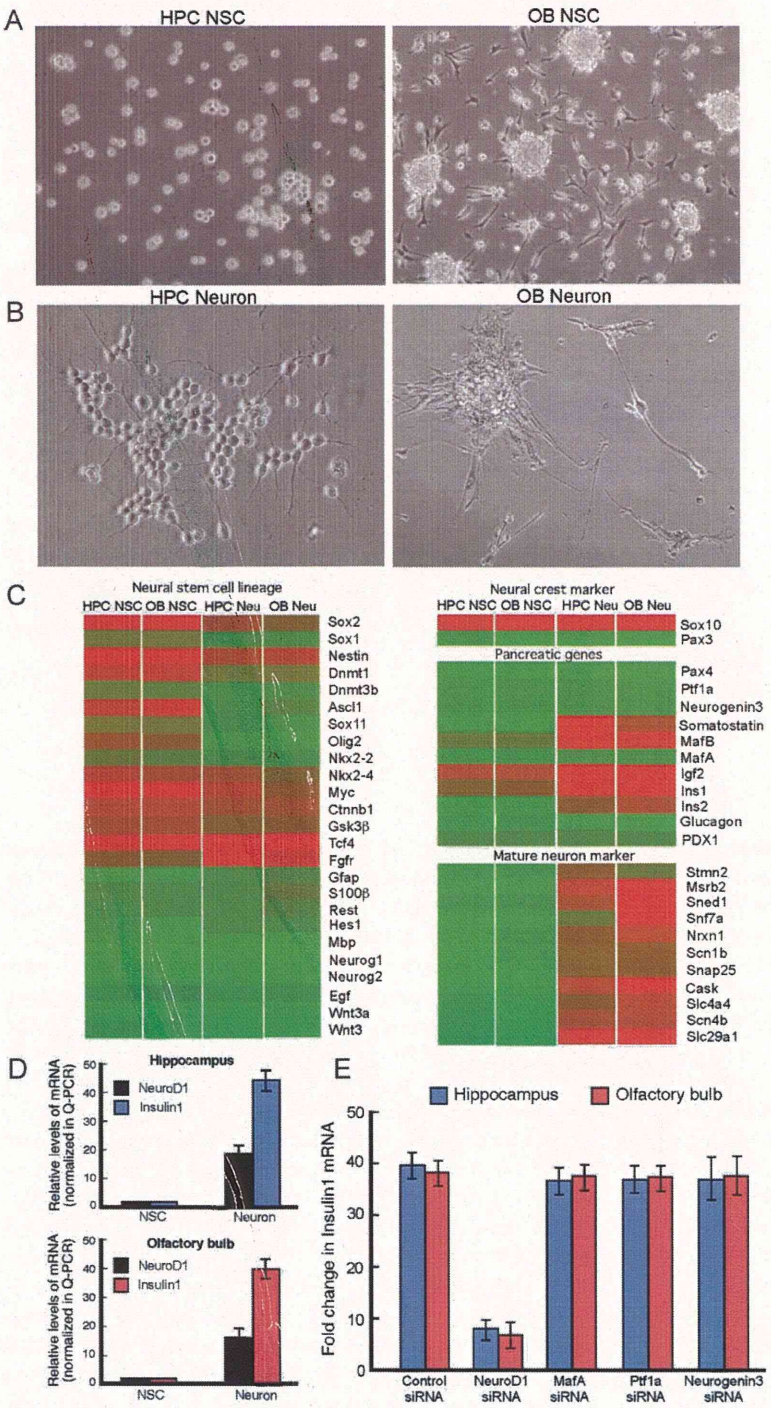

Figure 3. Adult NSCs derived from HPC and OB give rise to neurons expressing insulin.

A. The adult NSCs isolated from HPC and OB. Culture image of the proliferating hippocampal NSCs (HPC NSC, left) and NSCs derived from OB (OB NSC, right) of 7- to 8-week-old female Fisher 344 rats.

B. *In vitro* differentiated adult HPC- and OB neurons. When the culture was exposed to neuron differentiation conditions (RA + FSK + KCl), both HPC and OB cells extended neuritis (HPC neuron, left; OB neuron, right).

C. Gene expression profiles of HPC NSC, OB NSC, HPC neuron and OB neuron that were measured using Agilent rat genome microarrays. Typical genes for neuronal cell lineages, neural crest marker, pancreatic genes and mature neuron marker were analysed and the heat map using average-linkage hierarchical clustering is shown.

D. Induction of expression levels of insulin in HPC- and OB NSCs differentiating into neurons. The expression levels of proinsulin 1 and NeuroD1 were determined by Q-PCR analysis. Each mRNA value was normalized to GAPDH and then plotted.

E. Down-regulation of the neuronal expression of proinsulin 1 mRNAs with NeuroD1 siRNA. The neuronal induction of proinsulin 1 mRNA using siRNAs for NeuroD1, MafA, Pdx1 or Neurogenin 3 in HPC and OB neurons was examined in qRT-PCR analysis. Contol siRNA (scrambled siRNA) was transfected similarly. For quantification, the level of the control siRNA in NSCs group was set at 1, and the experimental siRNAs in neurons were then normalized accordingly.

Regulation of insulin expression in OB and HPC neurons

Neuronal insulin expression required NeuroD1 but not MafA, Pdx1 or neurogenin 3 (Fig 3). For NeuroD1 induction, paracrine Wnt3 plays an essential role in HPC. We determined that OB NSCs and HPC NSCs responded similarly and in a dose-dependent manner to Wnt3a ligands (Fig S6A of Supporting information). Moreover, the Wnt antagonist Dickkopf1 (Dkk1) down-regulated the expression of the TCF/LEF reporter (Fig S6A of Supporting information). These data suggested that canonical Wnt signalling is regulated analogously in both adult HPC and OB NSCs *in vitro*.

We detected IGF-binding proteins in the comparative profile analysis of adult NSCs and neurons (Fig S5 of Supporting information and Tables 1–5 of Supporting information). Thus,

IGFBP-2, IGFBP-3, IGFBP-4, IGFBP-5 and IGFBP-7 were expressed at high levels in both HPC and OB neurons (Fig S6B of Supporting information). The up-regulation of TCF/LEF reporter activity by the Wnt3a ligand was significantly inhibited by IGFBP-4 (Fig S6C of Supporting information). Treatment with an IGFBP-4 (anti-IGFBP-4)-neutralizing antibody attenuated the IGFBP-4-dependent reduction of TCF/LEF-reporter expression (Fig S6C of Supporting information). We did not detect clear effects of IGF-2, suggesting a specific inhibitory effect of IGFBP-4 on Wnt signalling.

Wnt3a treatment induced activation of the NeuroD1 promoter (Fig S6D of Supporting information). The reporter assay revealed the negative action of IGFBP-4 against Wnt3a on the *NeuroD1* promoter (Fig S6D of Supporting information). The activation of the *insulin-1* promoter by Wnt3a and anti-IGFBP activity was confirmed in both adult OB and HPC NSCs (Fig S6E of Supporting information). Chromatin immunoprecipitation (ChIP) analysis indicated that Sox2, HDAC1, dimethylation of histone H3 lysine 9 (Met-K9) and heterochromatin protein-1 (HP1) were associated on the endogenous *NeuroD1* promoter, suggesting a repressive chromatin state in NSCs (control, Fig S6F of Supporting information). In contrast, acetylated histone H3 (Ac-H3) was detected bound to the NeuroD1 promoter locus upon the introduction of Wnt3a and anti-IGFBP-4 (Fig S6F of Supporting information). The treatment led to associations of β-catenin, TCF4, dimethylation of histone H3 lysine 4 (Met-K4) and CREB-binding protein (CBP), indicating active NeuroD1 mRNA expression (Fig S6F of Supporting information). Similar complexes were detected in studies on chromatin remodelling of the E-box sequence region (Naya et al, 1997) on the insulin promoter (Fig S6G of Supporting information). Furthermore, the association of NeuroD1 with the *insulin* promoter was detected (Fig S6G of Supporting information). These data indicate that Wnt signalling promoted *insulin-1* expression via NeuroD1 activation in HPC and OB NSCs.

Wnt/β-catenin-signalling adult NSCs are required to generate pancreatic insulin-producing cells

Although neurons prepared *in vitro* and the native HPC and OB neurons expressed insulin, questions remained about whether adult NSCs can survive and potentially produce insulin within the pancreas. Although Wnt3 was produced in pancreatic α cells (Fig 2A), it is unknown whether adult NSCs respond to the Wnt3 in the pancreas. We, therefore, transplanted adult NSCs into the pancreas. We employed the Rosa-GFP mouse line to trace the fate of transplanted cells, which were transduced with Sox2^{Cre}GFP (retrovirus-encoding Sox2 promoter-driven Cre/GFP; Fig S7A of Supporting information). Furthermore, to examine Wnt signalling, we prepared adult HPC NSCs from β-catenin-conditional 'floxed' mice (Fig S7A of Supporting information). A retrovirus encoding Sox2^{Cre}GFP was infected to trace the fate of Sox2+ adult NSCs.

Adult NSCs were microinjected into adult mouse pancreas. Three weeks later, mice were injected with BrdU daily for 10 days. In the control (Control NSC TP), Sox2^{Cre}GFP+ cells co-localized with insulin (Fig 4A), C-peptide (Fig S7B of Supporting information) and NeuroD1 (Fig S7C of Supporting information). Interestingly, we found that Sox2^{Cre}GFP+ cells expressed MafA (Fig 4C) and pancreas transcription factor 1a (Ptf1a; Fig 4D). In microarray analysis (Fig 3C), adult NSCs did not express pancreatic β cells markers such as *MafA*. During embryonic development, lineage commitment of endocrine progenitors requires PTF1a (Kawaguchi et al, 2002). NSCs grafted in the pancreas, expressed β cell-specific markers such as PTF1a and MafA, suggesting that adult NSCs possessed the intrinsic ability to express these β cell-specific markers and that their expression levels were modulated by extracellular factors.

In β-catenin cKO NSC transplants (β-catenin cKO NSC TP), GFP+ cells decreased compared to that in control NSC TP mice (Fig 4F). Although Sox2^{Cre}GFP+ cells were detected, they did not express insulin (Fig 4B). Marker-positive cells with NeuroD1, PTF1a and MafA were rare in β-catenin cKO NSC TP mice (Fig 4G and Fig S7E of Supporting information). Sixty percent of Sox2^{Cre}GFP+ cells became insulin+ and C-peptide+ (control, Fig 4H). The proportion of (BrdU+ GFP+)/total GFP+ cells was higher in controls than in β-catenin cKO NSC TP mice (Fig 4I). Furthermore, the proportion of (insulin+ GFP+)/total GFP+ cells in β-catenin cKO NSC TP mice was 86% less than that in controls (Fig 4G). Some downstream β-catenin cKO NSC cell lineages were nestin+ (Fig 4E) and GFAP+ (Fig S7D of Supporting information). Since nestin is a neural progenitor marker (e.g. radial stem-like cells) and astrocytes specifically express GFAP, we hypothesized that grafted adult NSCs lacking the ability to respond to Wnt signalling remained in an undifferentiated state or possibly underwent glial differentiation.

Because GFP+ and BrdU+ GFP+ cell numbers in β-catenin cKO NSC TP mice were decreased (Fig 4F and H), we evaluated the presence of dead/dying cells by determining caspase 3 (AC3) expression by IHC. Apoptotic AC3+ cells were more abundant in β-catenin cKO NSC TP mice (Fig 4J and Fig S7F of Supporting information), indicating that Wnt/β-catenin signalling in Sox2+ NSCs was important for their survival. These data demonstrated that transplanted adult NSCs generated insulin-producing cells in the pancreas and that Wnt/β-catenin signalling played a critical role in the cell survival and function of *de novo* insulin biosynthesis in adult NSCs microinjected into the pancreas.

Diabetes therapy by transplanting adult NSCs

Next, we examined the potency of NSCs for treating diabetes *in vivo*. In the Control TP experiment (Fig 4J), AC3 was detected in microinjected adult HPC NSCs. Therefore, a collagen sheet was prepared to avoid needle wounds within the digestive pancreas. Adult NSCs were successfully maintained on the collagen sheet (Fig S8A of Supporting information), and we detected insulin expression in neuronal progenitors (NPs, cells committed to the neuronal lineage by 24 h culture under neuron differentiation conditions, Fig S8B of Supporting information). To analyse whether glucose regulated insulin secretion (i.e. C-peptide release), we treated cells with low or high glucose concentrations (2.5 or 27.5 mM, respectively). Intracellular C-peptide levels were detectably increased in both HPC and OB NSCs (Fig S8C of Supporting information).

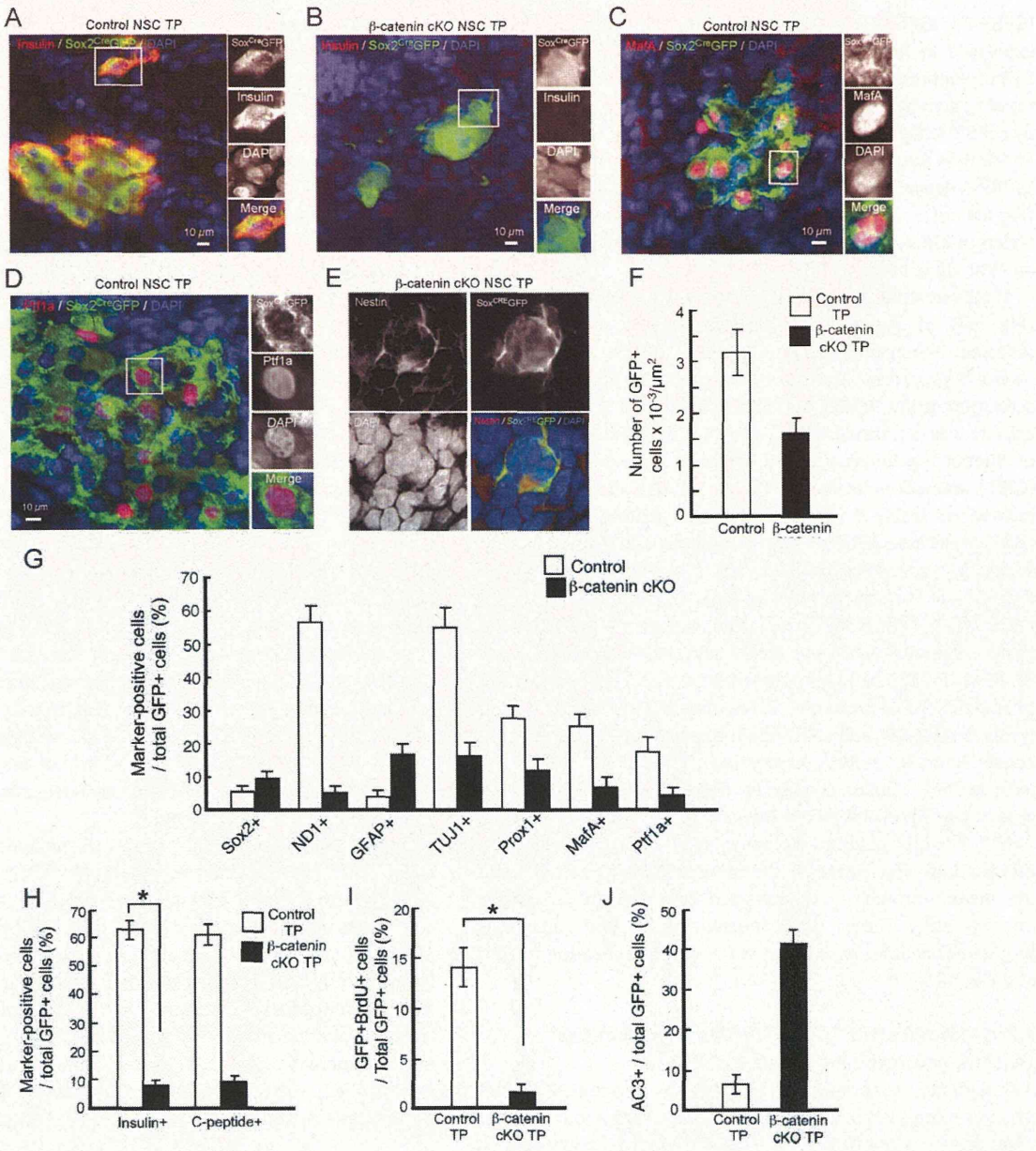

Figure 4. Transplantation of adult NSCs into the pancreas.

A. Adult HPC NSCs grafted into pancreas express insulin. IHC of tracing Sox2^{Cre}GFP cells. In control NSCs transplantation (Control NSC TP), Sox2^{Cre}GFP+ cells co-localized with insulin.

B. Adult HPC NSCs grafted into pancreas express insulin. IHC of tracing Sox2^{Cre}GFP cells. In β-catenin cKO NSCs transplantation (β-catenin cKO NSC TP), Sox2^{Cre}GFP+ cells were insulin-negative. Cells in the white square region are magnified and shown in separate panels at right. Insulin, red; Sox2^{Cre}GFP, green; DAPI, blue.

C. Detection of MafA-positive cells in grafted adult HPC NSCs into pancreas. IHC of MafA and Sox2^{Cre}GFP in control NSC TP is shown. MafA, red; Sox2^{Cre}GFP, green; DAPI, blue.

D. Ptf1a-expressing cells in grafted adult HPC NSCs into pancreas. Ptf1a, red; Sox2^{Cre}GFP, green; DAPI, blue.

E. IHC of tracing Sox2^{Cre}GFP cells in β-catenin cKO NSC TP. The β-catenin cKO NSCs remained in the nestin+ progenitor stage. Nestin, red; Sox2^{Cre}GFP, green; DAPI, blue.

F. Numbers of GFP+ cells in the pancreas of control TP mice (white bars) and β-catenin cKO NSC TP mice (black bars).

G. The phenotypic characterization of the grafted adult NSCs of control TP mice and β-catenin cKO NSC TP mice.

H. Numbers of marker and GFP double-positive cells in the grafted pancreas of control TP mice and β-catenin cKO NSC TP mice.

I. Percentages of BrdU and GFP double-positive cells in the grafted pancreas of control TP mice and β-catenin cKO NSC TP mice.

J. Numbers of AC3 and GFP double-positive cells in the grafted pancreas of control TP mice and β-catenin cKO NSC TP mice.

Adult HPC and OB NSCs were prepared from type I (STZ-induced DB rats) and type II DB rats (GK/slc DB rats) and were transplanted back into the pancreases of type I and type II DB rats, respectively. During 2 weeks *ex vivo* culture of NSCs, insulin expression was examined following Wnt3a and anti-IGFBP-4 addition. Although the HPC of DB animals contained higher IGFBP-4 and lower Wnt3 levels than wild-type (Fig 2D), Wnt3a and anti-IGFBP-4 treatment during the *ex vivo* culture rescued insulin expression (Fig 5A). These HPC and OB NPs were infected with a retroviral CAG promoter-driven EGFP expression vector to trace the grafted cells (Zhao et al, 2006). GFP+ NPs were transplanted into the pancreas of 8-week-old DB rats. Three to five collagen sheets were stacked and grafted near the splenic lobe among the three pancreatic lobes (i.e. the splenic, gastric and duodenal lobes, $n = 8$ *per* group), and blood glucose levels were recorded. Seventeen weeks after the transplantation, rats were injected with BrdU daily for 10 days.

The blood glucose levels of GFP-labelled HPC NP DB and OB NP DB transplants on collagen sheets were significantly reduced (Fig 5B and Fig S8F of Supporting information) and accompanied by up-regulated plasma and pancreatic insulin levels (Fig S8D and E of Supporting information). Nineteen weeks after transplantation, grafted OB NP DBs were insulin+ (Fig 5C, white arrows indicate GFP+ insulin+ grafts, and the arrowhead indicates an endogenous islet expressing low levels of insulin). We removed stacked cell sheets from splenic lobes 15 or 19 weeks after transplantation (Explant; Fig 5B and Fig S8F of Supporting information) to verify that the grafted GFP NPs were solely responsible for reducing blood glucose levels. We found that blood glucose levels increased ($n = 4$ *per* group of explant surgery), demonstrating that the grafted NPs produced insulin in DB rats.

To determine whether grafted adult NPs contributed to regulating glucose metabolism, we compared the animals' responses to glucose by measuring blood glucose level kinetics after transplantation. Animals transplanted with HPC NP DB and OB NP DB efficiently cleared glucose (Fig 5D). Furthermore, GFP+ cells expressing insulin were labelled by BrdU (Fig 5E), suggesting that the grafted cells proliferated. These data indicated that regulated insulin secretion by the grafted adult NPs from DB HPC and OB contributed to glucose homeostasis in the host DB rats.

DISCUSSION

Redundancy is a key feature of evolution that enables the conservation of efficient mechanisms; the most common manifestation of redundancy is exemplified by proteins that serve multiple purposes within the same cells at different developmental stages or in different cell types or tissues. Our analysis revealed that adult NSCs became insulin+ in the adult brain and in NSC-injected pancreas. The grafted NSCs reduced blood glucose and up-regulated insulin levels. NPs derived from OB and HPC produced insulin functionally via the support of Wnt3 (Fig 5). In embryonic pancreatic development, GFAP expression, representing the α cell population, was observed in cells derived from embryonic day 11 (E11) murine pancreatic buds (Fig S9A of Supporting information, left panel), where no TUJ1-positive cells, representing a β cell population, were detected. This indicated dominant α cell generation. In E17, TUJ1-positive cells (β cells), were generated on the α cell layer (Fig S9A of Supporting information, right panel), indicating that α cell generation preceded β cell generation in pancreatic development. In contrast, most cells derived from E11 murine brain stained positive for TUJ1 (Fig S9B of Supporting information, left panel). GFAP expression was restricted almost completely to the E11 brain, indicating that neuronal cell generation predominated, consistent with another report (Namihira et al, 2009). In E17, both TUJ1- and GFAP-positive cells were found (Fig S9B of Supporting information, right panel). Delayed gliogenesis in the embryonic brain has been demonstrated to result from methylation of the *GFAP* promoter (Takizawa et al, 2001). ChIP analysis indicated that GFAP expression responded to LIF stimulation (Nakashima et al, 1999) in E11 pancreatic buds but not in the E11 embryonic brain (Fig S9D of Supporting information). In E17, GFAP promoter methylation was detected at low levels in both the embryonic brain and pancreatic buds (Fig S9C of Supporting information). In adults, restricted GFAP expression was not observed in either HPC or pancreas (Fig S9C and D of Supporting information). These data suggest that the regulatory mechanisms that create Wnt3-secreting astrocyte or α cell niches are similar in the pancreas and HPC, at least in the adult stages, whereas, embryonic lineage commitment differs.

Our present study also suggested that the balance between the stimulatory actions of Wnt3 and the inhibitory actions of IGFBP-4 was regulated by DB status. IGFBPs modulate bioactivities of IGFs (Firth and Baxter, 2002), and IGF-1 and IGF-2 have been suggested to stimulate pancreatic islet cell growth (Le Roith, 2003; Liu, 2007). In the adult HPC, insulin/IGF expression facilitates NSC differentiation into the oligodendrocyte lineage (Hsieh et al, 2004) and enhances neuronal survival (Cheng and Mattson, 1992; Doré et al, 1997; Lindholm et al, 1996). IGF overexpression in transgenic mice results in brain enlargement and an increase in its myelin content (Carson et al, 1993; Ye et al, 1995). IGFs attenuate IGFBP-4 function when exogenously supplied to differentiating cardiomyocytes (Zhu et al, 2008). In diabetes, IGF-1 and IGF-2 were down-regulated along with *Wnt3* in both adult HPC and the pancreas (Fig 2C and D). These findings suggest that IGFBP-4 competitors (IGF-1 and IGF-2) were down-regulated in diabetes. Under normal conditions, insulin was expressed with the help of Wnt3, although IGFBP-4 was present. We hypothesize that endogenously expressed IGF-1 and IGF-2 control IGFBP-4 under normal conditions in both tissues. However, when DB status proceeds to a point where up-regulated IGFBP-4 and reduced IGF-1 and IGF-2 are observed, each factor likely further inhibits Wnt3-mediated signal transduction.

NeuroD1 is among the critical target genes of Wnt/β-catenin signalling in the adult stage. Sox2+ adult NSCs cannot express insulin when Wnt/β-catenin signalling is blocked endogenously (Fig 4), since adult NSCs with deleted *β-catenin* cannot trigger *NeuroD1* expression. The deletion of *NeuroD1* in adult HPC

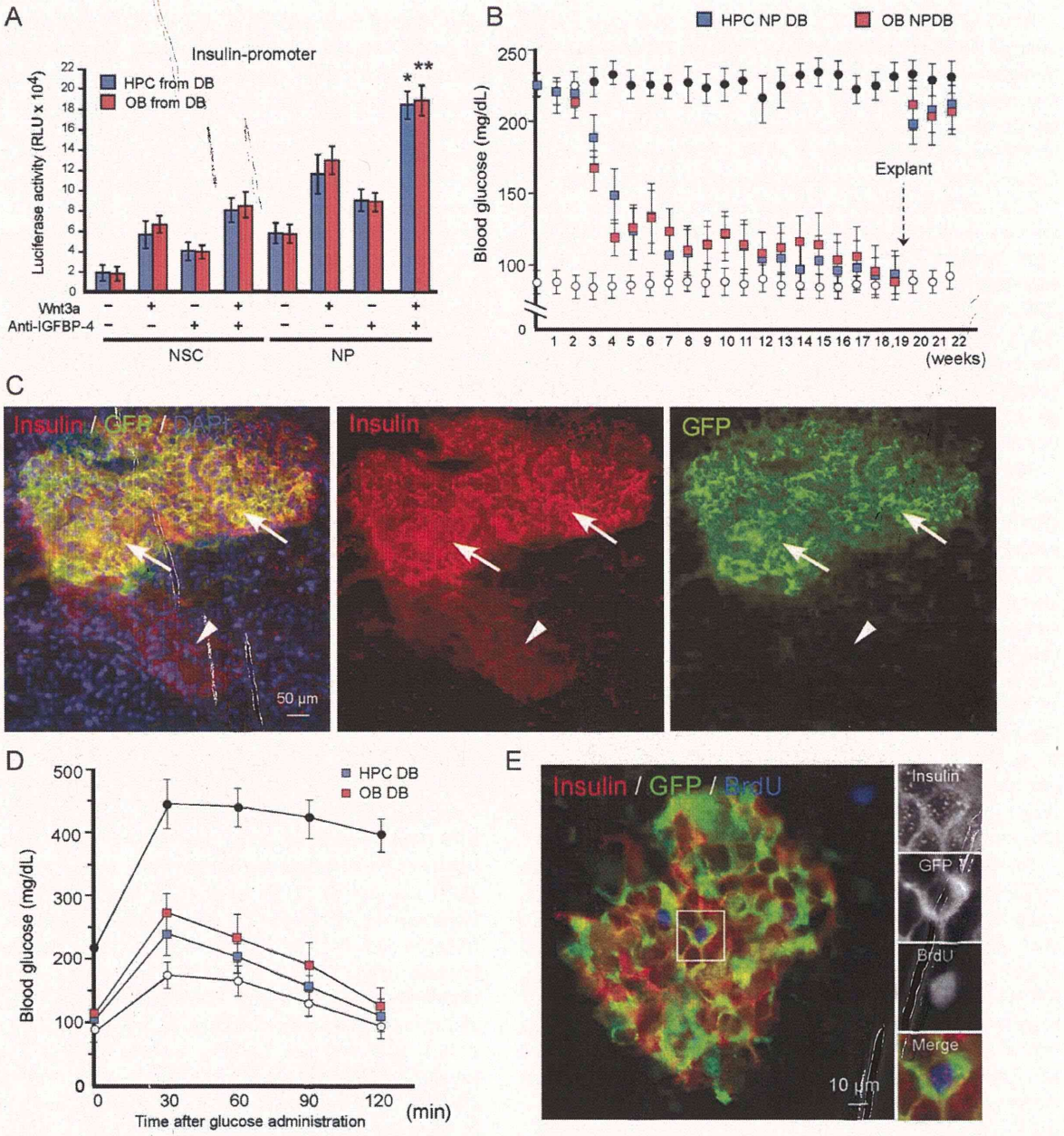

Figure 5. Therapeutic treatment of diabetes by adult NSC transplantation.

A. Insulin expressions in HPC and OB NSCs derived from DB rats. Insulin promoter activity was measured by using the luciferase reporter construct in adult HPC and OB NSC cultures that were prepared from type II DB rats [GK/slc rats, male; HPC from DB (blue bars) and OB from DB (red bars)]. The effect of Wnt3a ligand and anti-IGFBP-4 on the reporter was assessed in both undifferentiated NSCs and the NP cells. $^{*}p < 0.01$ and $^{**}p < 0.001$.

B. The effect of the grafted adult NPs in DB animals. HPC and OB NPs from type II diabetes rats were prepared *ex vivo* under treatment with Wnt3a and anti-IGFBP-4, and the resultant HPC NP DB and OB NP DB were transplanted into the pancreas of diabetes rats. Open circles, normal rats control; blue squares, HPC NP DB; red squares, OB NP DB; closed circles, diabetes GK/slc rats.

C. IHC of tracing CAG promoter driven EGFP cells (OB NP DB) in type II GK/slc DB rats. Co-localizing cells for insulin and GFP are indicated by white arrows. The preexisting islet expressing insulin at lower levels is indicated by the white arrowhead. Insulin, red; CAG-GFP, green; DAPI, blue.

D. Average of blood glucose levels in the response to intraperitoneal glucose tolerance test. Eighteen weeks after the implantation of adult NPs into rat pancreas, blood glucose levels were measured to glucose administration. Open circles, wild-type rats; blue squares, HPC NP DB grafts into DB rats; red squares, OB NP DB grafts into DB rats; closed circles, GK/Jcl DB rats. $n = 4$ *per* each group.

E. IHC of tracing HPC NP DB cells in DB rats. Cells in the white square region are magnified and shown in separate panels at right. Insulin, red; CAG-GFP (GFP), green; BrdU, blue.

results in decreased survival and maturation of newborn neurons (Gao et al, 2009). The diabetes-dependent impairments of adult hippocampal neurogenesis and synaptic plasticity might result from the diminished Wnt signalling that leads to *NeuroD1* down-regulation. Because *NeuroD1* is important for activating insulin mRNA expression, the decline in Wnt/β-catenin signalling in diabetes may impair *de novo* insulin mRNA expression by attenuating *NeuroD1* expression.

Our present study revealed that adult HPC and OB NSCs possess the intrinsic ability to generate insulin-producing cells via Wnt/β-catenin signalling. Since the successful isolation of NSCs from human adult OB was first reported, OB NSCs have attracted considerable attention as an accessible source of NSCs for studying various diseases. Adult HPC and OB NSCs derived from DB animals retained the ability to produce insulin in *ex vivo* culture (Fig 5). We further determined that the best source of insulin supply for transplantation into DB animals was adult NPs that had been committed into early neuronal lineage and had been treated with anti-IGFBP4 and Wnt3a to rescue their impaired Wnt signalling in DB animals. Grafted adult HPC and OB NPs reduced blood glucose levels for more than 2 months in DB rats (Fig 5B).

Various cell-based approaches have been explored for diabetes treatment: (1) differentiation to the β cell lineage from embryonic stem cells and/or induced pluripotent stem cells (iPS cells) (Lumelsky et al, 2001; Tateishi et al, 2008; Zhang et al, 2009), (2) direct conversion of differentiated cells into β cells (Thorel et al, 2010; Zhou et al, 2008) and (3) trans-differentiation of adult progenitor cells (Seaberg et al, 2004). This study provides an example of the direct use of adult stem cells from one organ to another without introducing inductive genes. Using adult NSCs for treating diabetes is potentially advantageous because donors are not required, the introduction of inductive genes is not necessary, and extracellular and endogenous regulation suitably resembles that employed by adult islet endocrine cell lineages. Although further studies, including the validation of other adult NSCs, should be forthcoming, the basic strategy outlined here should be useful for preliminary treatment of diabetes using the patient's own NSCs before the disease progresses.

MATERIALS AND METHODS

Cell preparation and culture

Female 7- to 8-week-old Fisher 344 rats with a body weight of 100–150 g were used (Charles River Japan, Inc). All animal procedures were performed according to a protocol approved by the Institutional Animal Care and Use Committee (IACUC) of the National Institute of Advanced Industrial Science and Technology. Adult NSCs were prepared and maintained as described previously (Dictus et al, 2007; Gage et al, 1995). The studies are described in more detail in the Supporting information.

In situ hybridization

Brains were dissected from freshly euthanized Fisher 344 rats and put in ice-cold saline until blocking. Brains were then placed in plastic blocks in insulin OCT (TissueTek) and frozen. Sections were cut at 15 μm by cryostat (LEICA CM1850. Leica). Brain sections on the slide-glass were hybridized with labelled riboprobes as described in more detail in the Supporting information.

Enzyme-linked immunosorbent assay of insulin

The insulin content of brain, HPC, femoral muscle, pancreatic head and pancreatic tail was measured by ELISA. Liquid nitrogen snap-frozen tissues of each age (7-week-old and 16-month-old Fisher 344 rats) were immediately homogenized and immunoreactive insulin was determined using rat insulin ELISA kit (Shibayagi, Gunma, Japan) according to the manufacturer's protocol. For details, see the Supporting information.

DNA Microarray

Total RNA from HPC/OB was extracted using ISOGEN (NipponGene) and labelled with Cy3. Samples were hybridized with Whole Rat Genome Microarray (G4131F, Agilent). Each sample was hybridized with the one colour protocol. Arrays were scanned with a G2505C Microarray Scanner System (Agilent). Data analysed by using GeneSpring GX11.0 software (Agilent). Two normalization procedures were applied; first, signal intensities less than 1 were set to 1. Then each chip was normalized to the 75th percentile of the measurements taken from that chip. Baseline transformation of those data did not perform. Genes with 'present' and 'marginal' flag value in all samples were used for analyses (32,622 genes). GO terms enriched with *p*-value cut off of 0.1 are extracted. The raw microarray data were submitted to the Gene Expression Omnibus (GEO) microarray data archive (http://www.ncbi.nlm.nih.gov/geo/) at the NCBI (accession numbers GSE27956).

Immunohistochemical analysis (IHC)

Immunofluorescence studies were primarily performed as described previously (Kuwabara et al, 2009): mouse monoclonal-beta tubulin-III (TUJ1; 1:500; Promega), guinea pig anti-insulin (1:300; Sigma), goat anti-C-peptide (1:250; Linco Research), goat anti-NeuroD (1:100; Santa Cruz), guinea pig anti-GFAP (1:500; Advanced Immunochemical Inc.), mouse anti-glucagon (1:300; Immuno), goat antibody to Wnt3 (1:100, Everest), mouse antibody to nestin (BD Biosciences), rat anti-BrdU (1:250; Abcam) and DAPI (Wako). All secondary antibodies were obtained from Jackson ImmunoResearch. The images were analysed using a Carl Zeiss LSM confocal imaging system (LSM 510; Carl Zeiss, Tokyo, Japan) or Olympus FV1000-D confocal microscope (Olympus Corporation, Tokyo, Japan).

Microscopic analysis and quantification

Microscopic analysis and quantification were completed as previously described (Kuwabara et al, 2009). Slides were coded during IHC analysis, and the code was not broken until after analysis was complete. Briefly, quantification of cell number within the DG of HPC was performed using the 20X objective of a Carl Zeiss LSM confocal imaging system (LSM 510; Carl Zeiss) or Olympus FV1000-D confocal microscope (Olympus Corporation) by an observer blind to experimental groups. Wnt3+, Insulin+, GFP+, BrdU+ and AC3+ cell quantification and morphology phenotyping were completed in every 12th 40-μm coronal section throughout the SGZ and outer portion of the GCL of the DG (bregma, −0.80 to −4.20 mm). Phenotypic analysis and co-localization of GFP+ cells with various markers in the DG were

The paper explained

PROBLEM:

The number of patients receiving care for type 1 and type 2 diabetes has more than doubled since the past decade. In type 1 diabetes, the patient's immune system aberrantly destroys the insulin-producing β cells of the pancreas. Type 2 diabetes is caused by insulin resistance, progressively reaching the point where β cells can no longer produce enough additional insulin. Cell replacement therapy can be an effective strategy to treat diabetes; however, insufficient supply of β cells from human organ donors is a major issue. Using stem cells as a potential source for deriving new β cells in a safe and easy way has long been awaited for.

RESULTS:

We demonstrated that subpopulations of neurons and adult NP cells express insulin in the brain. Adult NSCs, derived from the HPC and OB, give rise to insulin expressing cells. Adult NPs from DB rats could still generate insulin-producing cells, and the process requires the activation of NeuroD1 transcription factor via Wnt3 signalling. Under normal circumstances, insulin-expressing cells of neuronal lineage do not express phenotypic markers of pancreatic β cells. However, after transplantation into the pancreas, these neuronal cells not only increase their production of insulin but also start to express several transcription factors characteristic for pancreatic beta cells. As an approach to stem cell therapy that could be applied without gene transfer techniques, we supplied adult NPs from DB rats into the pancreases of DB rats. We found that this treatment induced insulin expression, reduced blood glucose levels and up-regulated insulin levels. Removal of these implants led to elevated levels of blood glucose, indicating that transplanting neural progenitor/stem cells into the pancreas could be a useful approach for treating diabetes.

IMPACT:

Our data indicate that adult NSCs are a relevant and safe cell source of insulin-producing cells. OB-derived NSCs are particularly useful because of their easily accessible location and their ability to generate insulin-producing cells, as hippocampal NSCs do. The findings of this study indicate the potential value of this technique for treating human diabetes without gene transfer, and would contribute as a novel strategy to overcome donor issues in cell replacement therapy of diabetes.

done on randomly assigned coronal sections throughout the SGZ using a confocal microscope (Carl Zeiss LSM confocal imaging system; 40X objective). Carl Zeiss Confocal Software was used for scanning, optical sectioning in the Z plane and 3D rendering.

Chromatin immunoprecipitation (ChIP) and qRT-PCR

ChIP was performed essentially according to the manufacturer's protocol by using a commercial kit (Upstate). Briefly, DNA was cross-linked to protein with formaldehyde. Cellular lysate was obtained by scraping, followed by pulse ultrasonication to shear cellular DNA. Immunoprecipitations were performed with 1.0 μg of antibodies and bound DNAs were purified by phenol:chloroform extraction. Resultant purified DNAs were analysed using quantitative PCR as described above. For details, see the Supporting information.

Animals

For the IHC analysis, we used 8- to 10-week-old C57/BL6 mice, 7- to 12-week-old adult female Fisher 344 rats, 3- to 4-week old young adult Fisher 344 rats, GK/slc type II DB rats and STZ- (70 mg/kg injectable dose; Wako) induced diabetic Fisher 344 rats (Type I diabetes model; 10-week-old females). The studies are described in more detail in the Supporting information.

Statistics

Experiments were analysed for statistical significance using a Student's t test, with all error bars expressed as ± standard error of mean (s.e.m.). Values of $p < 0.05$ or $p < 0.001$ were considered significant.

Author contributions

TK, MNK, FHG and MA conceptualized and designed the experiments; TK, MNK, YO, YI, MW and KT did the experiments; TK, MNK, YI, TS, KN and FHG analysed the data and prepared the manuscript.

Acknowledgements

We thank Takahisa Ohtake, Takahiro Numabe and Hideto Takimoto for providing assistance in the care of animals and in the experiments. We thank Mary Lynn Gage for editorial comments. TK, YO, YI, MW, KT and MA were supported by various grants from AIST. TK was partly supported by Suzuken memorial foundation and the Grant-in-Aid for Young Scientists (B). KN and TS were supported by the Foundation for Nara Institute of Science and Technology.

Supporting information is available at EMBO Molecular Medicine online.

The authors declare that they have no conflict of interest.

For more information

SCRC web page:
http://unit.aist.go.jp/scrc/cie/index_en.html

